

1 **Title Page**

2 **Exhumation History and Tectonics across Purulia – Bankura Shear Zone:**
3 **Constraints from Apatite Fission Track Analysis.**

4 Amal Kumar Ghosh

5 Department of Physics, Bhagwant University, Ajmer – 305 004

6 Email: ghosh.971@gmail.com

7 **Abstract**

8 The Purulia-Bankura Shear Zone (TPSZ) is a ductile- to-brittle-ductile, tectonically disturbed narrow zone of
9 nearly 150 Km with a WNW-ESE trend. Two different rock assemblages, the Chhotanagpur Gneissic complex
10 and rocks of the Shinbhum Group (SG) Occur on opposite sides of this shear zone The TPSZ borders the
11 Meso- Proterozoic greenschist facies litho-package of the SG, which is comprised of meta sedimentary rocks,
12 felsic volcanics, mafics/ultramafics, granitoids and an alkaline/carbonatite suite of rocks. The Chotanagpur
13 Gneissic Complex contains amphibolites to granulite facies in the north mafic-ultramafic suites of rocks that
14 are in close proximity to felsic volcanics, suggesting a bimodal character of magmatic episodes. The TPSZ was
15 subjected to a compressional regime, and its development is attributed to thrusting and wrenching. The area
16 initially underwent rifting, volcanism, granite plutonism, and shallow sedimentation followed by shearing. The
17 possible reactivation and exhumation history of the area was analyzed using apatite fission tracks (AFT). Offset
18 of AFT ages between the two rock assemblages occur on the two sides of this shear zone, indicating that
19 reactivation occurred due to over-thrusting at approximately 500 Ma, which is further supported by the results
20 of thermal history models. The youngest AFT age of 260 Ma means that this age is a result of the entire thermal
21 history of the sample. Furthermore, samples from Sushina hills indicate AFT ages decreasing towards Beldih
22 via Chirugora. We interpret this to be an effect of motion along this shear zone. The thermal history indicates
23 that the samples were rapidly exhumed at 600 Ma, given that the samples were cooled rapidly and subsequently
24 re-heated; therefore, a cooling-only history is impossible. Denudations are predominantly controlled by tectonic
25 processes and to a lesser degree, by erosional processes. Most of the sample ages are in the 200-to 300 Ma
26 range, but their track-lengths are quite short, providing thermal history information before 600 Ma .

27 **1. Introduction**

28 A state of stress may influence a development of the basins, especially intraplate stress. This stress could be
29 compression stress which could produce relative uplift of the basin flank, subsidence at the basin centre, and
30 seaward migration of the shoreline. Increasing the level of tensional stress however, induces widening of the basin,
31 subsidence of the basin flank, and thus causes landward migration of the shoreline (Kooi and Cloetingh, 1992).
32 Therefore, a rifting activity which involves crustal stretching by tensional stress either acceleration of subsidence
33 would certainly give effects to the basin flank and shifting of the shoreline.

34 Continental rifting cannot be solely regarded as a responsible factor for repeated faults reactivation and uplift.
35 Another factor which triggers the faults reactivation may be derived by the latest phase of pre-drift extension
36 (Redfield et al. 2005).

37 Subduction carries fluids, sediments, oceanic crust, and offscraped continental crust towards the Earth's interior,
38 and may cause accretion and magmatic activity. These processes lead to forearc deformation, faulting, mountain
39 building, and ultimately to continental growth and destruction. In addition, all continental margins also experience
40 erosion, which is controlled by climate, tectonic uplift, and the development of morphology (Burbank 2002, Bonnet
41 and Crave 2003).

42 Erosion is a mechanism that enables exhumation and, more generally, vertical movements of rocks within the crust
43 (Ring et al, 1999, Willet et al. 2003).

44 Thus, for a full understanding of margin dynamics, information on the timing and kinematics of deformation from
45 the rock record has to be linked with quantitative constraints on exhumation histories of individual geologic units
46 within a marginal basin.

47 A shear zone is regarded as a planar zone of concentrated, dominantly simple shear deformation and accommodates,
48 partly or wholly, an imposed regional or local strain rate, which the country rock cannot accommodate by bulk
49 deformation (Ramsay, 1980; Rmsay and Huber, 1983, 1985). The shear zone is thus a general term for a relatively
50 narrow zone with sub-parallel boundaries in which shear strain is localized. Most shear zones rise from depth
51 commonly taking the basement rocks up to the surface.

52 The Singhbhum Group of rocks and the Chhotanagpur Gneissic Complex (CGC) that belong to distinct geological
53 domains are in contact with each other along a tectonically distributed dislocation zone , viz. Purulia-Bankura Shear
54 Zone or the Tamar-Porapahar Shear Zone (TPSZ), located to the north of Singhbhum Shear Zone (Fig. 2). A marked
55 tectonic control is evident in the disposition of this shear zone as they are restricted to the peripheral zones of the

56 cratonic area (CGC) bordering the Singhbhum Group of rocks. The WNW-ESE lineament is marked to have
57 extended from Porapahar in the East in the district of Bankura to Tamar in the West in the district of Ranchi through
58 Sushina, Chirugora, Kutni, Mednitani and Beldih in the district of Purulia.

59 The tract of TPSZ is exposed in the surface by almost continuous signature of cataclastic movement resulting in
60 brecciation, grinding, fracturing, shearing, mylonitisation indicating the nature of disturbance along this zone. At
61 places, this shear zone passes either through rocks of Singhbhum Group or Chhotanagpur Gneissic Complex. Several
62 parallel (sympathetic) shears are developed between the Dalma volcanic and the Tamar Porapahar Shear Zone. The
63 formations north of Archaean cratonic margin (Singhbhum Granite Complex) and south of the Chhotanagpur
64 Granite Gneissic Complex are now referred as 'North Singhbhum Mobile Belt'(NSMB), which evolved during
65 Proterozoic.

66 The five well-developed zones in the Eastern Singhbhum lose their identity in the western part. The Chaibasa
67 Formation and Dhalbhum formation are folded into overturned 'Singhbhum Anticlinorium' and Dalma
68 Synclinorium' with E-W trending sub-horizontal axis. The southern (overturned) limb of the anticlinorium is
69 sheared and overthrust upon the younger rocks of Iron Ore Group in the south. This overthrusting has given rise to a
70 major shear zone which is termed 'Copper Belt Thrust' or Singhbhum Shear Zone'. The area adjoining the shear
71 zone throughout the belt are affected by three phases of deformation. This shear zone consists of number of thrust
72 planes with variable upward displacement of the northern block (Naha, 1994 Lind references therein). A number of
73 cross faults are also known to have displaced the shear zone.

74 From the structural pattern worked out in different parts of Chhotanagpur Granite Gneiss Terrain, it is seen that the
75 rocks of the area bear imprints of three generations of deformations producing distinctive folds and related linear
76 and planar fabrics. The rocks of CGC have witnessed several period of magmatism, tectonism, sedimentation,
77 metamorphism, partial melting and mineralization.

78 Thus, the intense deformation in CGC and SSZ and the thrust sense of movement of northern block(CGC) towards
79 south over southern block(Singhbhum Group) point to a complex exhumation history. Again, the rocks of TPSZ had
80 suffered brecciation, grinding, deeper fracturing and intense shearing. The development of the basin may be
81 attributed to the thrusting and wrenching (A. Acharyya et al.,2006). Hence, it is unknown to what extent the TPSZ

82 was affected by the intense deformation in the area adjoining this shear zone and how this might have been
83 influenced by the number of cross faults which have displaced the SSZ.

84 Thus, TPSZ is a particularly well-suited area to study long term margin evolution and mass transfer patterns. The
85 present fission-track reconnaissance study in the TPSZ addresses several key topics of current interest The core aims
86 of this study are to understand the burial and exhumation history of Purulia - Bankura Shear Zone (TPSZ). It is also
87 attempted to determine the timing of possible vertical movement of the TPSZ. The possible reactivation could be
88 reflected by an offset of Apatite Fission Track (AFT) ages between two tectonical rock assemblages. Another
89 objective of this study is to unravel the thermal histories of the rocks in the study area, to obtain new insight in the
90 exhumation history. To meet these we conducted an apatite fission track thermochronology study because fission
91 track analysis yields age information on low-temperature increments of the cooling history of rocks. Given the
92 thermal history of the upper crust is well constrained, fission track ages may provide quantitative estimates on
93 erosional and tectonic exhumation, on tectonic movements at fault zones, and on the thermal evolution of
94 sedimentary basins (Gallagher et al. 1998 and references therein).

95 **2.Geological setting**

96 The Eastern Indian shield is well known for the Archean cratonic batholith of Singhbhum granite (3.2 – 2.7 Ga)
97 encircled in the north by Dalma greenstones (1.6 Ga, Sakar & Saha, 1962), which is a part of the 200-km long, 50-
98 km wide, North Singhbhum Mobile Belt (Fig.1). The North Singhbhum Mobile Belt (NSMB) is delimited in its
99 southern periphery by the famous Singhbhum Shear Zone (SSZ) that is characterized by intense ductile
100 shearing/thrust with rich copper-uranium mineralization. The thrust belt affects a host of rock types, including the
101 Singhbhum Group, the Iron Ore Group (IOG), and the Dhanjori volcanics. The NSMB in its northern margin has a
102 tectonic boundary with the Chhotanagpur Gneissic Complex (CGC) along the Tamar-Porapahar (TP)
103 lineament/South Purulia Shear Zone. The lithological assemblage south of the CGC represents suites of the
104 Singhbhum Group (Fig. 1). In the Purulia and Bankura districts, the CGC is composed largely of migmatites, granite
105 gneiss, psammite, calc-granulite, amphibolite, and metadolerite with small granulatic patches of khondalite,
106 charnockite and anorthosite, which in turn is intruded by granite and mica pegmatites of later ages. Along the shear
107 zone alkaline, alkaline ultrabasic rock and carbonatite occur intermittently for approximately 35km. indicating their
108 close genetic relationship (Roy, 1941; Inogradov et al. 1964; Gupta et. Al., 1971, Bhattacharya, 1976; Roy Burman

109 and Nandi, 1978; Ghosh Roy and Sengupta, 1988; Banerji, 1988; Majumdar, 1988; Bhattachayra and Das Gupta,
110 1992).

111 The presence of quartz-kyanite and kyanitic rocks near both the shear zones signify that there were clay-rich
112 horizons. However, Sarkar et al. (1988) supported that the tectonic evolution of the CGC occurred as a consequence
113 of the subduction of the oceanic lithosphere of the Singhbhum micro-plate and the process continued upto the Late
114 Proterozoic. (2300 Ma – 850 Ma). The subducted block experienced subsequent prolonged geodynamic and
115 geochemical processes. In these metallogenic domains, zones of rifting and upward movement of mafic melts to the
116 surface with or without strong vertical displacement and horizontal compression led to the emplacement of Fe, Mn,
117 Cr, V, Ti, Au, U and asbestos (Banerjee, 1988; Deb and Roy, 1988). Gorumaheshani volcanics and associated
118 Banded Iron Formation occur in faulted blocks within the Singhbhum granite. These features are extensively
119 intersected by dykes of doleritic composition and intruded by V-Ti rich gabbro anorthosites. A resemblance to the
120 ophiolitic composition of Sukinda, Nausahi,

121 Bonai and Jujohatu volcanics (Banerjee 1988), and the anorthosite gabbro and granophyre intrusives in Singhbhum
122 suggest the occurrence of rifting.

123 During the Archean to the Early Proterozoic, mantle-derived metallogenic phase was dominant, which changed over
124 to a crust-derived metallogenic epoch towards the Middle Proterozoic in Singhbhum and adjoining parts of West
125 Bengal (Banerjee, 1988). The available geochronological data suggest that polymetallogenesis occurred in stages
126 mostly in the Early-Mid Proterozoic times approximately 1600 Ma (Fruncheteau et al. 1979; Bostrom and Peterson,
127 1965; Scott et al., 1974). Geochronological data are scarce from this Shear Zone. Felsic volcanics from Ankro
128 (approximately 8 km south of the SPSZ) has been dated to be 1500 Ma by the Rb-Sr whole rock method (Sarkar and
129 Ghosh Roy, 1999) and the same rock near Chandil, north of the Dalma Volcanics, yielded a Rb-Sr whole rock age of
130 1484 ± 44 Ma (Sengupta et al. 2000). Gabbro-Pyroxenite rock north of Dalma was dated to be 1619 Ma (Rb-Sr date,
131 Roy et al. 1999) near Kunchea.

132 The nature of the Shear Zone has been described as ductile to brittle-ductile (Pyne, 1992,
133 Bhattacharya, 1989, Acharyya and Ray, 2004). Shearing has been demonstrated to be syn to post-kinematic to F1
134 folds with concomitant development of mylonitic fabric. Mylonitic foliation has been found to act as the form
135 surface of F2 folds. Micro-structural study revealed a thrust sense of movement of northern block (CGC) towards
136 the south over the southern block (Singhbhum Group).

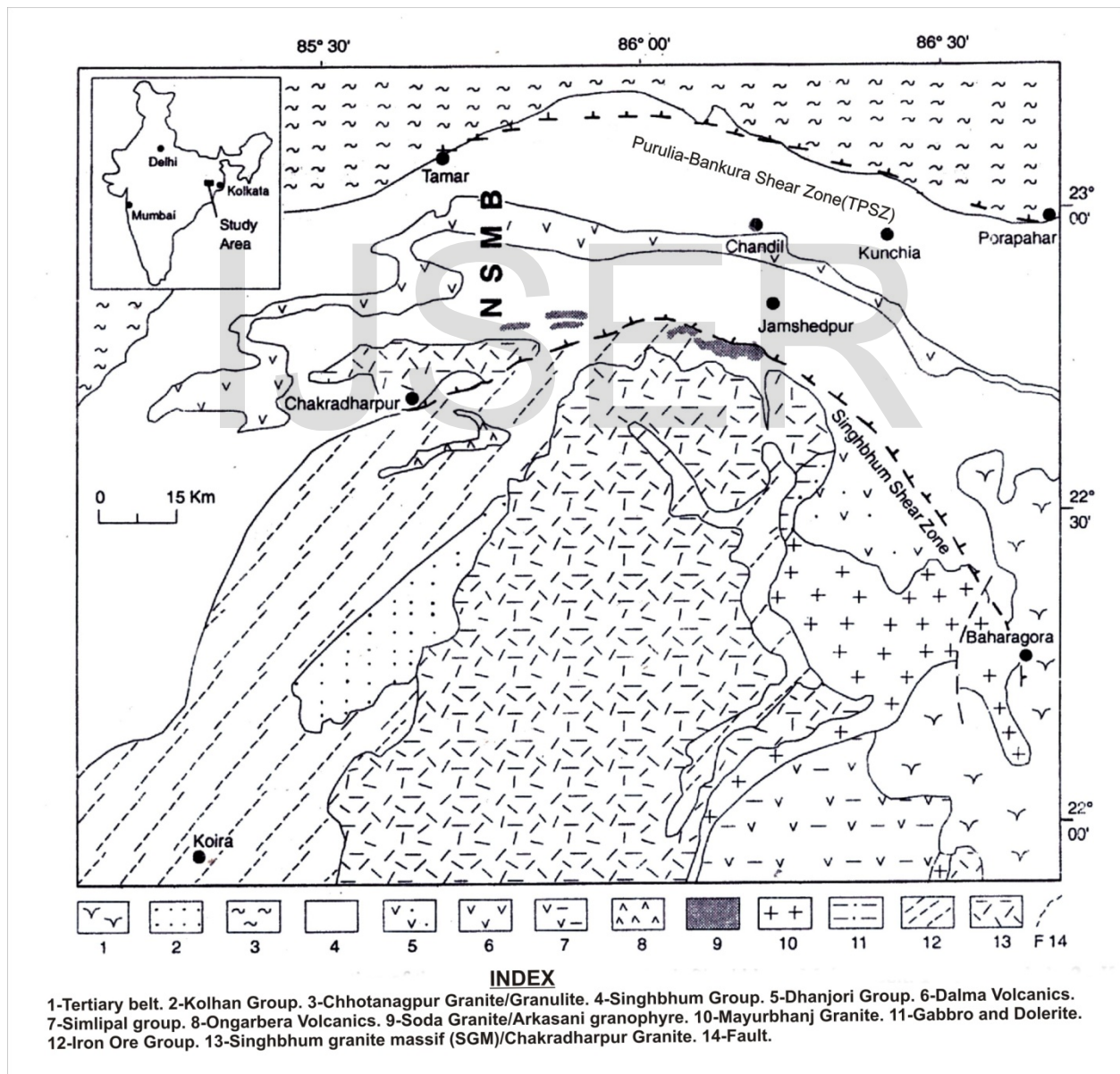
137 **2.1 Structural Features**

138 Quartz-reef/quartz-breccia/quartzite–mylonites are linearly arranged in low-lying as well as elevated ridge-forming
139 expressions (near Sarberiya) demarcating the pronounced lineament of the TPSZ. The composite S1 – S2 foliation
140 and mylonitic foliation are the dominant structural grains in the area. S1 parallels the mylonitic foliation, which also
141 acted as a form of surface to F2 folds, producing regional antiform and synform E-W axial trace. Shear Zones had
142 been developed syn to post-kinematic to F1. The entire packet of litho-assemblage from augen gneiss of CGC in the
143 north of the quartz mica-schist of the Singhbhum Group in the south bears imprints of ductile shearing. Shear
144 indicators such as C-C'/S-C-C' fabric are identified, in addition to downdip stretching lineations. The ductile shear
145 zone represents a pronounced thrust type of the movement tectonics demonstrated by clear-cut downdip stretching
146 lineation on the S1/mylonitic foliation plane in quartzite-mylonite, Biramdih gneiss, Felsic volcanics. A wide area
147 along the zone is markedly dominated by voluminous felsic volcanics, which were earlier described as phyllites and
148 schist. The mode of deposition of the facies A, B, or C might be due to the pyroclastic process, but compositional
149 homogeneity is a notable feature pointing against an admixed epiclastic process. The repetitive layers of the
150 tuffaceous volcanoclastic (Facies A) represent the variation in the pyroclastic facies B and C. In the course of
151 geological evolution of the lithopackage of this shear zone, successive emplacement of felsic volcanism and granite
152 plutonism was eventually followed by deposition of sedimentary litho-units such as quartzite mica-quartz schist and
153 metagreywacke.

154 After the rocks came into place, the basin started closing with an F1 folding deformation, which, during its
155 culmination stage, produced the shear zone. The shear zone is characterized by downdip stretching lineations on the
156 S1 foliation surface. Shear indicators present in ignimbrite quartzite and mylonite indicated thrusting of the northern
157 block towards the south over the southern block. The near horizontal fabric in the augen gneiss and granite mylonite
158 might suggest an additional tectonic component. The variation in tectonic fabric (downdip versus near horizontal)
159 may be explained as combining ductile thrusting and wrenching during progressive shortening of the area (Lagardo
160 and Michard, 1986). In the subsequent folding deformation event, the mylonitic fabric became folded and S1
161 foliation crenulated during F2 when regional antiform synforms with the E-W axial plane developed in the region.
162 A transition from the continental rift, developing into the incipient oceanic crust with continued lithospheric
163 stretching, may be suggested (A. Acharyya et al. 2006). There have been a number of tectonic models advocated for
164 NSMS (Sarkar, 1982, Sarkar et al. 1992; Bose; 1992). Bose (1992) opined that the entire setting resembles an

165 ensialic back arc basin. Gupta and Basu (2000) refuted the idea of back arc setting and indicated that it only takes
166 into account the second stage of Wilson's cycle without any reference to the first stage. It appears that the
167 intracratonic rifting and ensialic orogeny model proposed by Sarkal et al. (1992) and Basu (2000) for the mobile belt
168 (NSMB) also applies for the TPSZ. A. Acharyya et al. (2006) advocated that the migmatized mica schist occurring
169 as a marker all along the contact of CGC and SG might be representing an intracratonic crustal sag deposit. The
170 Manbazar schist belt also represents a Trans-dalma low grade supracrustal that branches off the SPSZ (toward the
171 northeast of Sindri) and again imply a crustal sag deposit (Mahadevan, 1992), which might have acted as a failed
172 arm for later rifting sequel. The Manbazar Schist belt remained protected most likely for the reason that it was
173 completely confined within the cratonic realm of the CGC. The crustal sags are suited for lithospheric weakness in
174 the Proterozoic crust. Rifting could be initiated in such locales of pre-existing weakness (Dunbar and Sawyer,
175 1988). The presence of high volume of magmatization along this shear zone, the arcuate shape of the lineament
176 following quartz reef, distinct tourmalinite, bands, absence of dyke, swarms etc. are all indicative of the rupture of
177 the crust. This Shear Zone is approximately 30km north of the Spine of the Dalma Volcanics. Litho-characters of the
178 Dalma range are typical of deep ruptures of a rift where oceanic crust had formed (report of pillow lava,
179 agglomerate, felsic tuff etc. are common). The margins of the rift should be shallower where silicic volcanism
180 abounds. A. Acharyya et al. assumed that the entire rift zone spans from the northern limit of the SPSZ to the
181 southern limit of the SSZ, with the Dalma range representing the deepest axis of the rift. Records from similar
182 settings in other parts of the world are also encouraging. In the Proterozoic Mid-continental Rift, U.S.A., the flows
183 are chiefly felsic ignimbrite and basalt (Allen et al. 1995). Even in a modern day rift setting, ignimbrites are the
184 predominant rock type (60% by volume), as recorded in the Oslo-rift (Neumann et al. 1995). The range of felsic
185 ignimbrite in the present setting includes dacite, andesite and rhyolite. In a similar trend, the San Pedro volcanic
186 craton produced multiple voluminous, heterogeneously mingled units (dacite-andesite, dacite-basalt-andesite-
187 rhyolite) indicating that shallow silicic magma chambers were repeatedly established and then intruded by new
188 inputs of mafic magma (Dungan et al. 2001). This behavior also implies that rifting was operative at the site of
189 ignimbrite ponding. Integrating the sequence of events along this Shear Zone, it essentially involves an initial
190 crustal sagging for the deposition of supracrustal, which is followed by the initiation of rifting in an ensialic resident
191 crust with the formation of narrow basin, primarily ponded with felsic volcanics and granites. This sequence was
192 followed by development of deeper fractures and pouring of mafic/ultramafic rocks, with the subsequent tapping of

193 syenites, alkali feldspar granites and carbonatites. The granite plutonism, felsic volcanism, boron effusion and
 194 pouring of ultramafic extrusive/intrusive happened to be the early phase of crustal tectonic activity, followed by
 195 shallow sedimentation (at places volcanogenic, epiclastic) occurring as veneers over igneous suites. The basin was
 196 then subjected to the compressional regime, and the development of the Shear Zone (TPSZ) may be attributed to the
 197 thrusting and wrenching along this lineament.
 198 Hence, a total sequence of basin initiation by rifting, volcanism, granite plutonism, sedimentation followed by
 199 shearing at the close of the basin is preserved in this setting. It would be appropriate to reconcile the Central Indian
 200 Tectonic Zone (CITZ) as presenting a magma-event in the Meso-Proterozoic of Indian peninsula.



201

202 **Fig. 1.**

203 **3. Method and sampling strategy**

204 Every solid material, once it is penetrated by nuclear particles, will obtain linear trails of disrupted atoms, which also
205 reflect damage on the atomic scale. Fission tracks are such a damage feature. The emerged features are produced by
206 spontaneous fission of ^{238}U (Gallagher et al, 1998). In general, fission track dating is similar to the other dating
207 methods that rely on the same equation of radioactive decay, i.e., estimating the abundance both of the parent and
208 the daughter isotope. In fission track analysis, the age corresponds to the number of ^{238}U atoms and the number of
209 spontaneous tracks per unit volume. To obtain the number of spontaneous tracks, we simply count the number of
210 spontaneous fission tracks on a given surface of a mineral grain. Meanwhile, the abundance of ^{238}U can be determined
211 by irradiating the samples with low energy thermal neutrons to induce fission of ^{238}U . By controlling the thermal
212 neutron flux, we obtain the number of 'induced tracks', which also signifies the abundance of ^{238}U . Because the
213 ratio of the $^{238}\text{U}/^{235}\text{U}$ is constant, we are able to estimate the abundance of ^{238}U (Gallagher et al. 1998).

214 Fission tracks are meta-stable features, i.e., the tracks can fade or be annealed. The annealing of the tracks can cause
215 the tracks to shorten. Therefore, length track distribution is a fundamental parameter in the fission track analysis.
216 Several factors that influence annealing are temperature, time, pressure, chemical composition and ionizing radiation
217 (Fleischer et al., 1965b). However, temperature combined with time is the greatest contributing factor for the
218 annealing. Therefore, the track length distribution contains information of the thermal history of the analyzing
219 samples (Gallagher et al., 1998). Recently, applications using fission track analysis are widely known to solve
220 geological problems. This thermo-chronology method is rather exceptional compared to other methods, whereas the
221 temperature dependence of the annealing of the fission tracks provides information of the thermal history. Various
222 geological problems can be unraveled by this method, such as the thermal history of sedimentary basins,
223 sedimentary provenance, the structural evolution of orogens, the continental margin development, and long-term
224 denudation on continents (Gallagher et al. 1998). Based on the kinetic indicators, AFT ages and track length data,
225 the thermal histories of seven samples were modeled using HeFT_v (Ketcham, 2013, Version 1.8.1). Forward
226 modeling was used to test the possible time-temperature paths indicated by the AFT ages and the track length
227 distribution. The start of the thermal history models for all samples considered was set to a nearly high temperature

228 constraint(near 600 Ma) keeping in mind a particular hypothesis to be tested. We took samples from two rock
229 assemblages that occur on the two sides of the shear zone, targeting a possible reactivation to be revealed. The
230 samples of BAP(S), BAP-20, and BAP-168, were collected from Beldih; CAP was collected from Chirugorah; and
231 SAP was collected from Sushina (Fig.2).These samples belong to the Singhbhum Group of rocks. The samples of
232 BAN-1 and BAN-2 were collected from Mochrakend, Majhia and Bangalipara, Majhia, respectively (Fig.2). These
233 samples belong to the West Bengal part of the CGC block. We took samples along the shear zone, e.g., BAP(s),Bap-
234 20,Bap-168, CAP and SAP to understand the effect of motion of the shear zone. A few general observations can be
235 made about the application of the approach to understanding exhumation. First, the evolution of exhumation is best
236 evaluated when samples are collected from a well-dated stratigraphic section that spans the exhumation event.
237 Second, a condensed section from the perimeter of the basin is most likely to preserve unrest detrital grains and
238 therefore provide provenance information. This problem is especially acute for apatite. Third, during erosion, the
239 removal of cover rocks or a 'deadzone' precedes the exposure of rocks with young cooling ages. Fourth, fast
240 exhumation results in a short lag time and slow exhumation results in a long lag time. In this study, a rapid
241 exhumation is exhibited by almost all of the thermal history models.

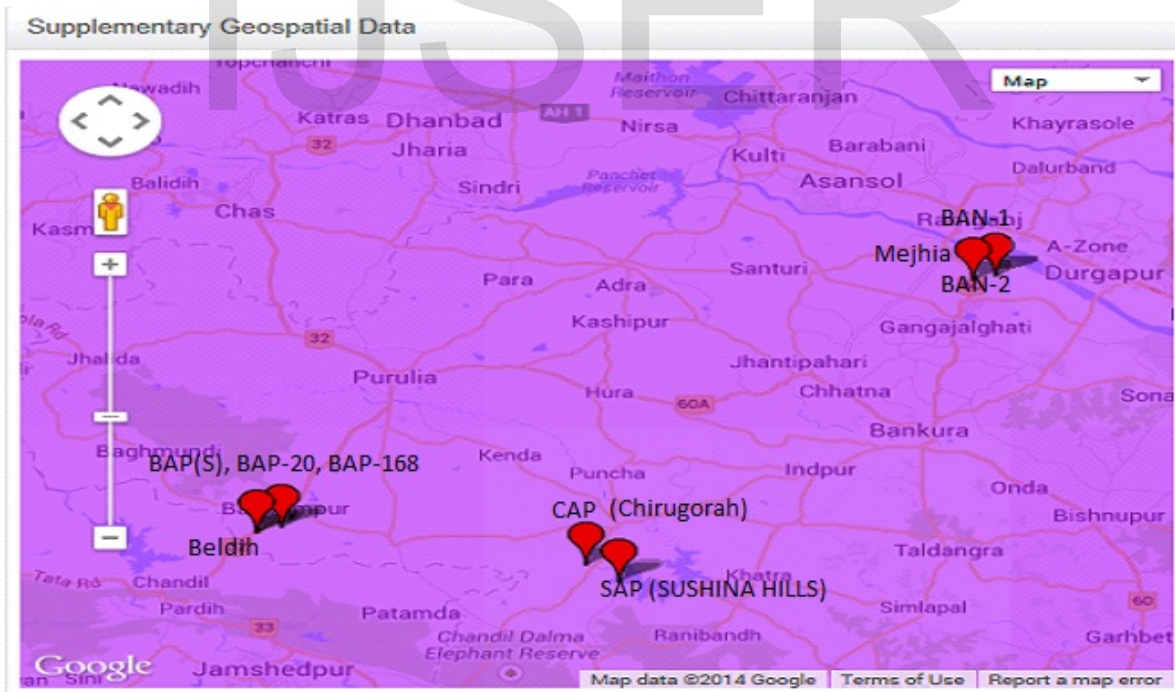


Figure 2: Location map of the studied area

242

243

244 **4. Discussion and Interpretation.**

245 Five samples from the Singhbhum Group of rocks and two samples from the Chhotanagpur Gneissic block were
246 analyzed, and the results are shown in table 1 (see also Appendix A).Seven thermal history models are also
247 discussed. Here, a possible exhumation history along this shear zone is proposed based on the AFT ages and the
248 thermal history. A minimum of 15 grains were selected to achieve a satisfactory age measurement. The large age
249 errors, e.g., 14.25 %, 12.76%, 11.05% and 10.85%, are found in samples SAP, BAP(s), BAN-1 and CAP,
250 respectively. As already known, low Uranium samples present a problem because of low induced track densities.
251 The P (X^2) test was performed to measure the Uranium variation in the samples. A value of P(X^2) larger than 5%
252 means that the grains are assumed to be a single age. Four samples, BAP(s), SAP, CAP and BAN, failed the X^2 test,
253 which may indicate bimodal distributions for the samples. Track length measurements were performed for seven
254 samples: five samples from Singhbhum Group (BAP(s), CAP, SAP,BAP-20 and BAP-168) and two samples from
255 Chhotanagpur Gneissic Complex (BAN-1 and BAN-2).The sample ages from the Singhbhum Group are in the 200-
256 300 Ma range, but the MTLs are quite short, so samples contain information on the thermal histories before 600 Ma
257 (Richard Ketcham, personal communication). The short track lengths indicate a possibly more complex thermal
258 history. The value of D par are dominated by low values in the range of 1.15-1.49 μm . Carlson et al. (1999) affirmed
259 that the D par value of less than 1.75 μm anneals rapidly, which is also typical for the near-end members of calcian -
260 fluorapatites. The fluorapatites member has been known to be less resistant to anneal than cl-apatite (Gleadow &
261 Duddy, 1081). According to Kelcham et al. (1999) the fission track with D par = 1.5 μm , cl = 0 wt%, experience a
262 total loss of tracks in the range of 100°C-110°C in the geological environment. Hence, it can be inferred that these
263 samples approximately have the properties of low Cl and OH, high F content and rapid annealing and are most
264 likely typical for Calcian-fluorapatites.

265

266 By applying apatite fission track analysis, the possible reactivation of the TPSZ was attempted to be revealed, which
267 could be reflected by an offset of the Apatite Fission Track (AFT) age between the two rock assemblages that occur
268 on the two sides of the shear zone. Seven thermal history models were also developed to unravel the thermal
269 histories of the rocks in the study area.

270 The AFT ages exhibit a significant difference between the two block, where as the samples that were taken from the
271 Singhbhum Group of rocks have AFT ages in the range from 260 Ma- 535 Ma, with a weighted mean age of 325.67
272 Ma (Carboniferous). Meanwhile, from the West Bengal part of the Chhotanagpur Gneissic Complex block is
273 obtained AFT ages in the range of 453.22 Ma -407.034 Ma with a weighted mean of 430.13 Ma (late Silurian-Early
274 Silurian time). Fault movements, which postdate the formation of particular profile of apparent fission track age
275 with depth, will disrupt and offset the apparent fission track 'stratigraphy'. Discontinuities may then be observed in
276 the regional pattern of the apparent ages, which will reveal the presence of such fault movements and place
277 constraints on the timing of the movement. The time represented by the youngest apparent age so revealed will place
278 a maximum constraint on the time of the fault movement. Quite apart from the time constraints, the observed fission
279 track pattern may provide valuable structural information, especially in rocks where no clear structural markers exist
280 (Gleadow). Interpreting the AFT age is very seldom a straightforward process. The youngest age "will place a
281 maximum constraint" on the timing and not provide an estimate for that timing (Richard Ketcham, personal
282 communication). In the case of all of my samples, the track lengths are shortened, which reduces the fission-track
283 age compared to a sample that has gone through no partial annealing. Thus, even though the youngest age of the
284 sample is 260 Ma, the event that offset it from rocks across the shear zone and/or brought it into the temperature
285 regime that allows fission tracks to be retained could have been much earlier. In our HeFTy models, seldom is an
286 "event" found that corresponds to the youngest age (260 Ma); in all cases where the lengths are substantially
287 shortened, the age (260 Ma) is a result of the entire thermal history of the sample, not just one instant in time. The
288 oldest mean AFT age indicates that the reactivation of TPSZ occurred due to over-thrusting near 500 Ma (Late
289 Cambrian time), which is further supported by the results of the thermal history models. For the reactivation
290 corresponding to near 500 Ma, the event that resulted in these rocks cooling enough to start retaining fission tracks
291 could have been much earlier. Further, the samples from Sushina hills exhibit an AFT age decreasing towards
292 Beldih via Chirugora. We interpret this behavior as an effect of motion along this shear zone. The result of the
293 thermal history model indicates that almost all of the forward models have rapid cooling from high temperature to a
294 surface temperature near 600 Ma. A very rapid cooling mainly subsequently occurred due to volcanic activity,
295 hydrothermal activity (Duddy et al. 1998), dyke displacement, faulting or meteorite impact (Miller & Wagner,
296 1979), and volcanic activity (Ketcham, personal communication). It is inferred that Exhumation caused reactivation

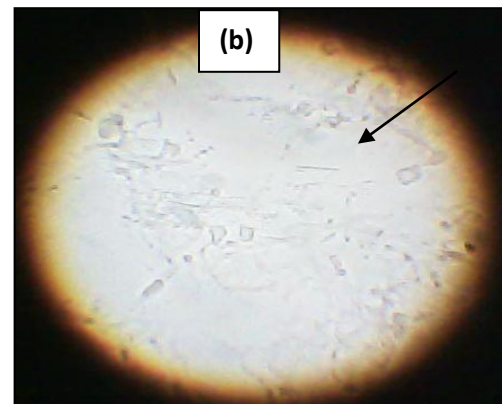
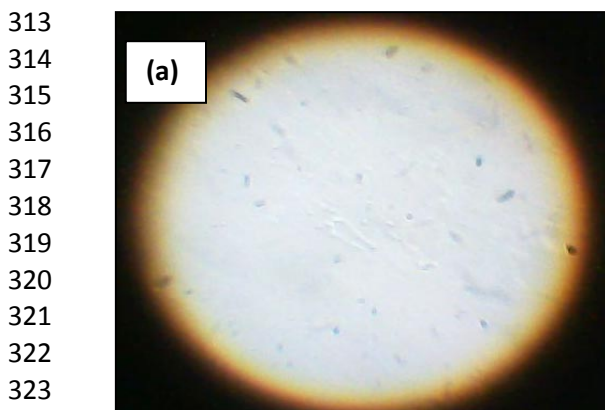
297 of this shear zone at 600 Ma due to volcanic activity. Samples are then re-heated near 500 Ma, which is referred to
298 as a burial event; it may also reflect over-thrusting near 500 Ma.

299 This age is in good accordance with the age of reactivation constrained from the AFT ages between the two rock
300 assemblages. As a result, the cause of reactivation may be attributed to the over-thrusting. Because the samples were
301 cooled and then re-heated, cooling-only history is impossible to obtain. The cooling event may be interpreted to
302 have occurred due to mainly a tectonic process.

303 In BAP-20, We have the present-day temperature at approximately 65 degrees. This sample was collected at depth
304 of 20m. It is most likely impossible to say definitely how many times the samples entered the PAZ. Moreover, the
305 hypothesis, e.g., the duration of the residence of the samples in the PAZ, cooling rate, linear or non-linear cooling,
306 over printing and bimodal distribution, are quite impossible to infer because the thermal history models indicate that
307 the samples are cooled rapidly and then re-heated. As a result, cooling-only history is impossible to determine.

308 **5. Apatite Description**

309 Generally, the whole samples display fair-good apatite quality. Several particular features on the apatite, however
310 could lead to possible errors in the counting. Typical features are; bad grain surface, wide cracks, zoning whereas
311 uranium is concentrated in clusters, thus the tracks are distributed unevenly on the grain, dislocations, and very low
312 or very high uranium content (Fig.3)



332
333
334
335
336
337
338
339
340
341
342
343
344
345
346

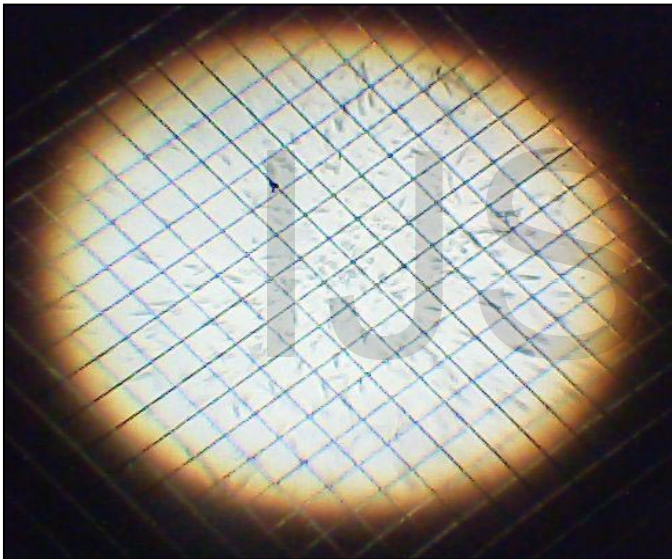
(c)



Fig.3: Several defect features occurred on my apatite samples. These defects lead to possible errors in the counting.

They are; (a) & (c) low uranium concentration results rare fission tracks, (b) dislocation features (marked by arrow)

347
348
349
350
351
352
353
354
355
356
357
358
359
360
361
362
363
364
365
366
367
368
369
370
371
372
373
374
375
376



377
378
379
380
381
382
383
384
385
386
387
388
389
390
391
392
393
394
395
396
397
398
399
400
401
402
403
404
405
406
407
408
409
410
411
412
413
414
415
416
417
418
419
420

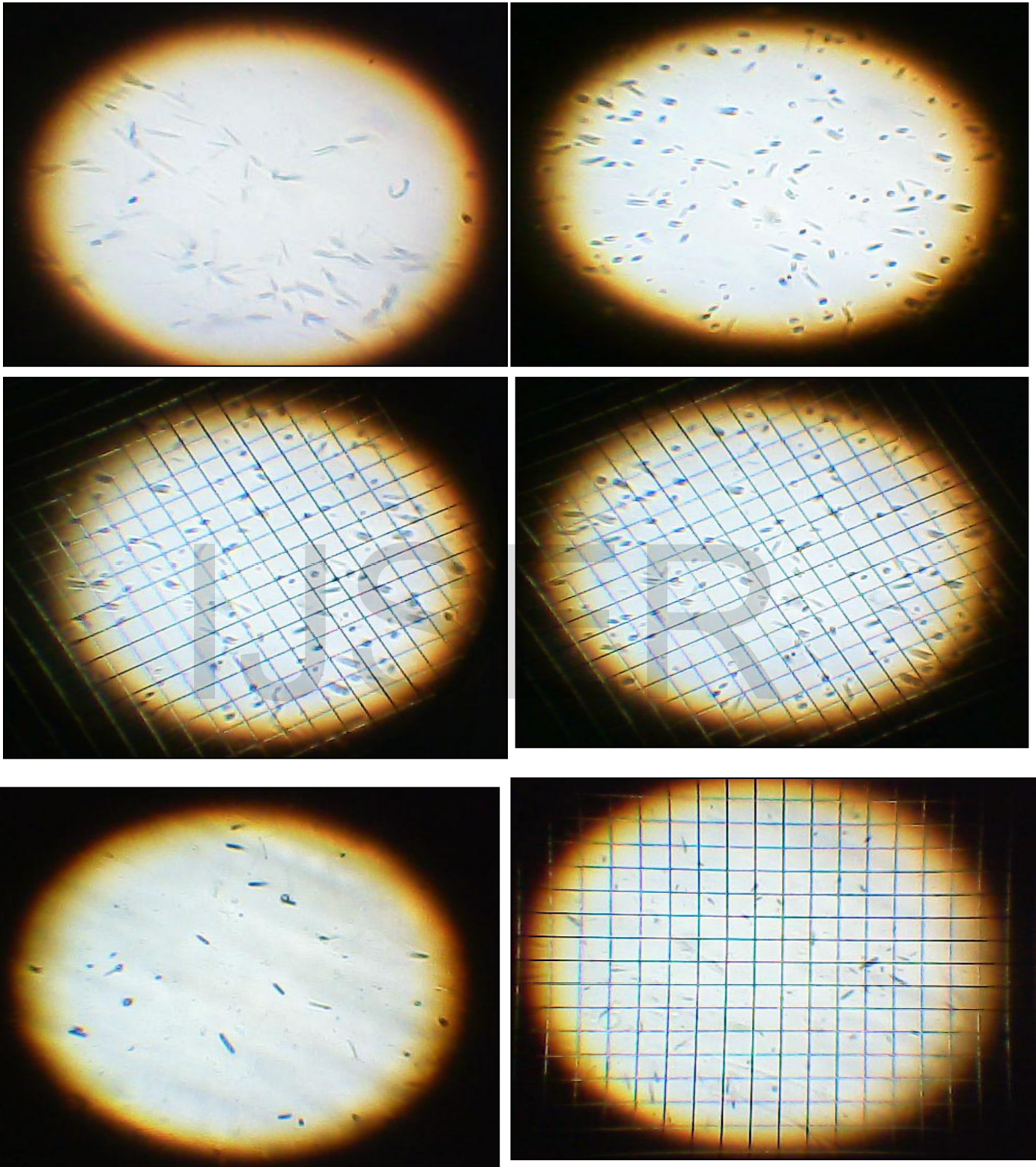


Fig.4. Induced Track Imprinted on Mica Sheet

422 Table-1

423 Results of AFT analyses : ages calculated using dosimeter glass IRMM -540R with 15ppm U, zeta = 250, irradiated at FRMII, calibrated by
424 traditional zeta approach and external detector method, N=Number of grains, ρ – track densities given in 10^5 tr cm^{-2} , ρ_d - dosimeter track density,
425 N_d – number of tracks counted on dosimeter, $\rho_s(\rho_i)$ – spontaneous (induced) track densities, $N_s(N_i)$ – number of counted spontaneous (induced)
426 tracks, $P(\chi^2)$ – probability for obtaining χ^2 value for n degrees of freedom, where n=no. of grain – 1, MTL – mean track length, SD – Standard
427 deviation.

Sample No.	Rock Type	Depth (m)	No. of Grains (N)	Dosimeter		Spontaneous		Induced		$P\chi^2$ (%)	U (ppm)	Mean Age (Ma)	MTL (μm)	SD	No. of Tracks	D_{par}	Error(%) on Mean Age
				P_d	N_d	P_s	N_s	P_i	N_i								
Singhbhum Group																	
BAP(S)	Breccia with fibrous apatite veins	NA	15	19.25	1232	0.98379	136	0.88975	123	0.64	0.42	260.51	11.01	NA	80	1.22	12.76
CAP	Apatite - Magnetite	NA	18	19.25	1232	1.2779	212	0.9645	160	2.23	0.45	306.96	10.99	NA	90	1.32	10.85
SAP	Syenite	NA	15	19.25	1232	3.25	156	1.45833	70	0.33	0.68	535.25	10.75	NA	80	1.191	14.52
BAP-20	NA	20	18	19.25	1232	3.67717	610	3.35768	557	11.64	1.56	281.56	9.84	NA	85	1.28	6.51
BAP-168	NA	168	16	19.25	1232	1.74967	258	2.00059	295	24.63	0.94	244.06	10.96	NA	75	1.49	8.98
West Bengal part of CGC Block																	
BAN-1	Granite	NA	15	19.25	1232	1.552	215	1.0706	148	3.29	0.50	406.70	10.46	NA	75	1.29	11.05
BAN-2	Granite	NA	15	19.25	1232	3.7109	513	2.5535	353	16.20	1.19	453.22	10	NA	75	1.19	7.48

428
429
430

431 6. Conclusion

432 The largest age error (14.52%) occurs in sample SAP. This high error is most likely due to a very low uranium
433 concentration (0.68 ppm). As already known, low uranium samples place limits on how robust the ages could be. In
434 low uranium samples, an exact match between the areas counted in the grains and the mica is often hard to achieve.
435 An adjustment by eye is difficult and subjective because the outline of the induced tracks on the mica does not
436 reflect the shape of the analyzed grain.

437 Track lengths were measured using a calibrated eye-piece graticule and stage micrometer with significantly poorer
438 resolution compared to digitizing tablet. The precisions of individual fission-track length and angle to c-axis
439 measurements are approximately $0.15\mu\text{m}$ (1σ) and 2° (1σ) respectively (Donelick 1991).

440 Measurements of etch pit diameters were carried out both the parallel (D_{par}) and perpendicular to the c-axis (D_{per}).
441 However, the values of D_{per} are ignored because of imprecise measurements reasons. It is unlikely to obtain an
442 accurate measurement of D_{per} using an optical microscope with the magnification which was used in this study.

443 A failure of a positive correlation between the AFT ages and the MTL occurred because the track length is
444 determined rather by the thermal history than the fission track ages. This occurs remarkably in complex cooling
445 histories, whereas the pre-existing tracks will be shortened in significant time. If cooling histories are more complex
446 thus also produce more complex length distribution (Gleadow et al., 1986).

447

448 In this study, we attempted to unravel the exhumation history in the Purulia - Bankura Shear Zone (TPSZ) by means
449 of a low temperature thermo-chronological technique, i.e., the apatite fission track analysis; we also attempted to
450 determine the patterns and timing of possible vertical movements along the TPSZ. This possible reactivation could
451 be reflected by an offset of the Apatite Fission track (AFT) ages between two distinct tectonical geological domains
452 that occur on the two sides of the TPSZ in combination with the structural data and the geological data. Another
453 attempt of this study was to unravel the thermal histories of the rocks in this study area to obtain new insight into the
454 exhumation and uplift history of the TPSZ.

455

456 Samples taken from the Singhbhum Group of rocks have AFT ages in the range from 260 Ma – 535 Ma,
457 with a weighted mean age of 325.67 Ma (Carboniferous). Meanwhile, the West Bengal part of Chhotanagpur
458 Gneissic block has AFT ages in the range from 453.22Ma – 407.034Ma, with a weighted mean of 430.13 Ma (Late
459 Silurian - Early Silurian time).The thermal histories have been modeled from seven samples: five samples from the
460 Singhbhum Group and two samples from Chhotanagpur Gneissic complex.

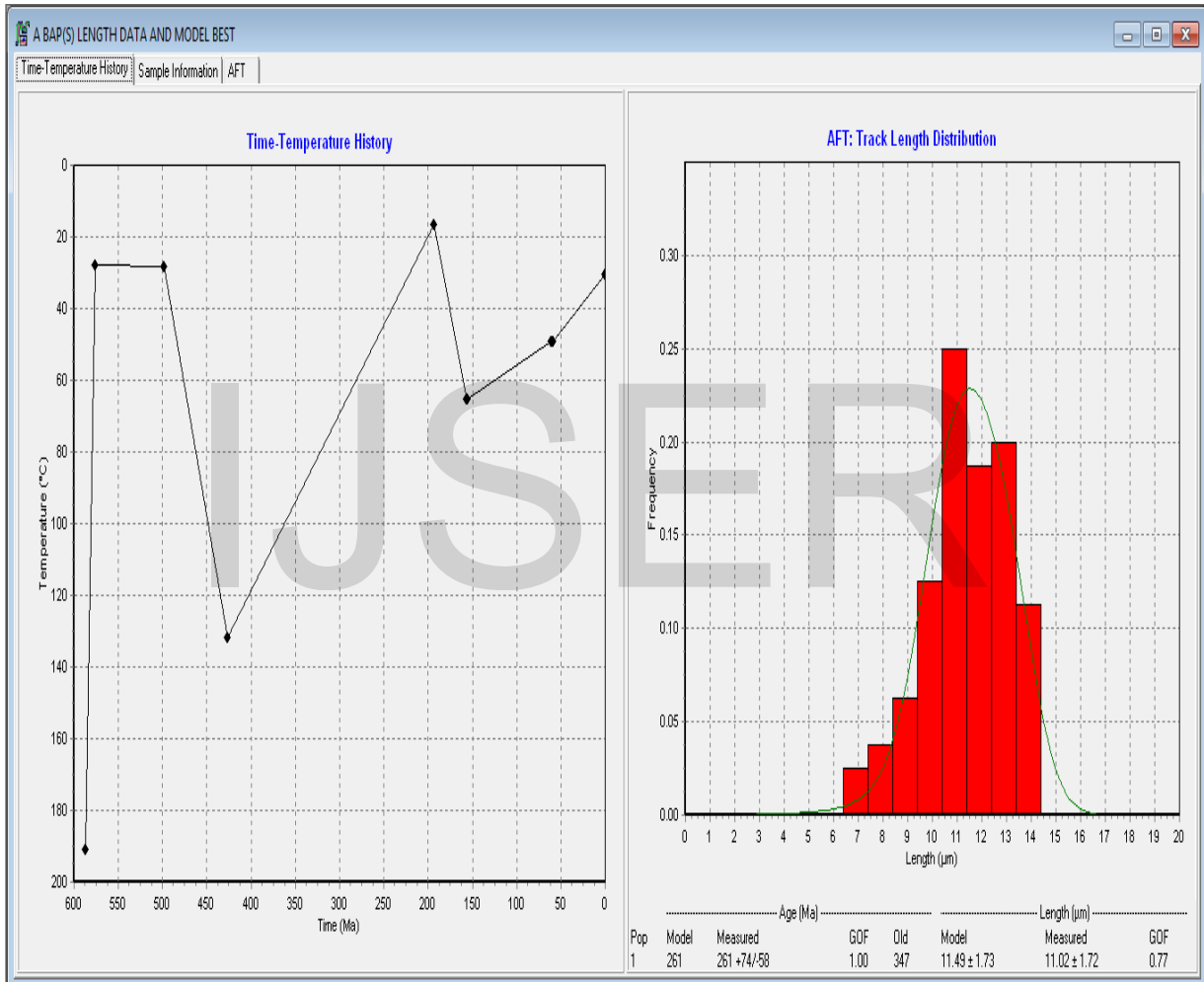
461

462 The thermal history models indicate that the cooling-only history is impossible to determine. The models
463 also indicate that samples contain information on the thermal histories before 600 Ma. The AFT ages of the samples
464 from the Singhbhum Group indicate the effect of the motion along the TPSZ. Exhumation due to volcanic activity

465 caused reactivation of the TPSZ at 600Ma. Denudation was dominantly controlled by a tectonic process and to a
 466 lesser degree by an erosional process.

467 The youngest age of the sample (260 Ma) is a result of the entire thermal history of the sample, not just one instant
 468 in time. The reactivation of the TPSZ occurred due to over-thrusting near 500Ma (Late Cambrian time).

469 **Fig.5(a). Thermal History Models from Singhbhum Group of Rocks**
 470



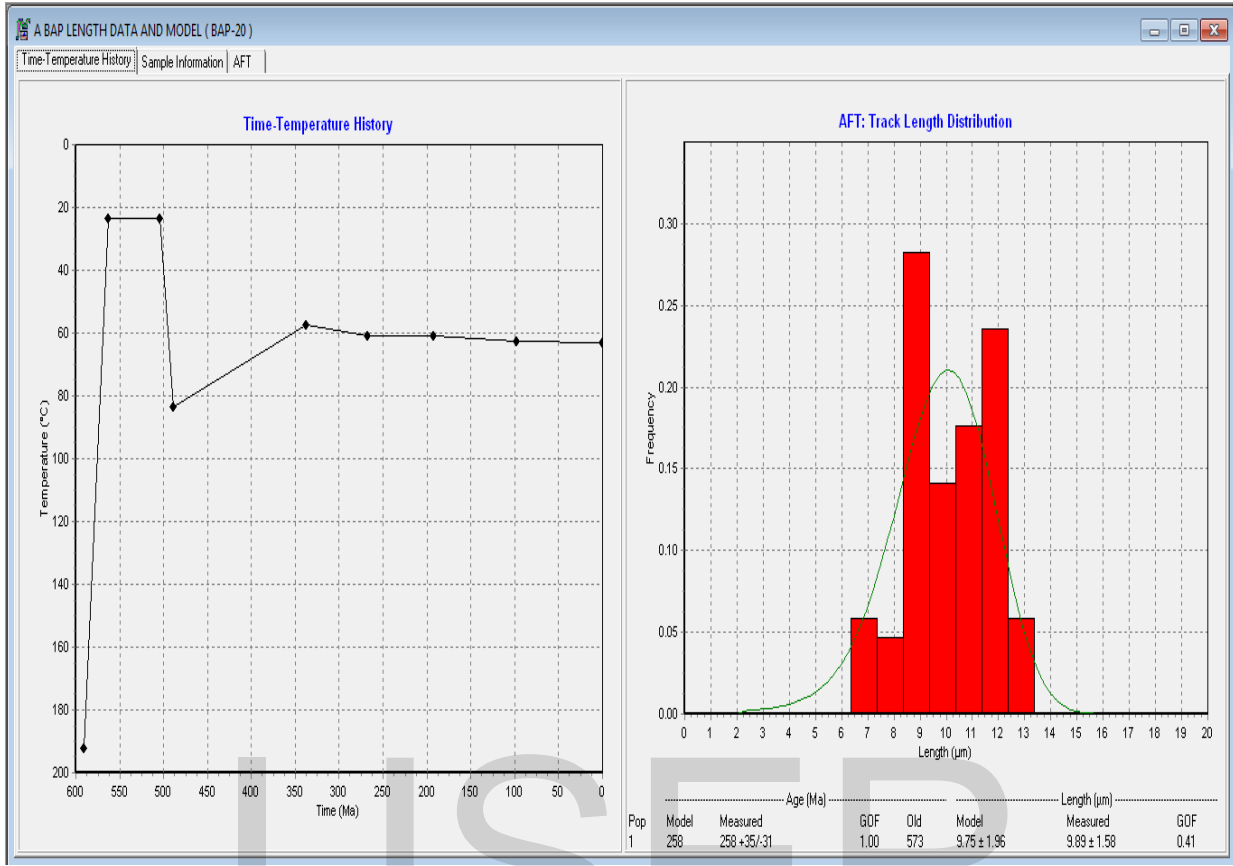
471

472

473

Sample Name: BAP (S)

Model: 261	Model: 11.49 ± 1.73 µm
Measured: 261 +74/-58	Measured: 11.02 ± 1.72 µm
GOF: 1.00	GOF: 0.77



474

475

476

477

478

479

480

Sample Name: BAP – 20

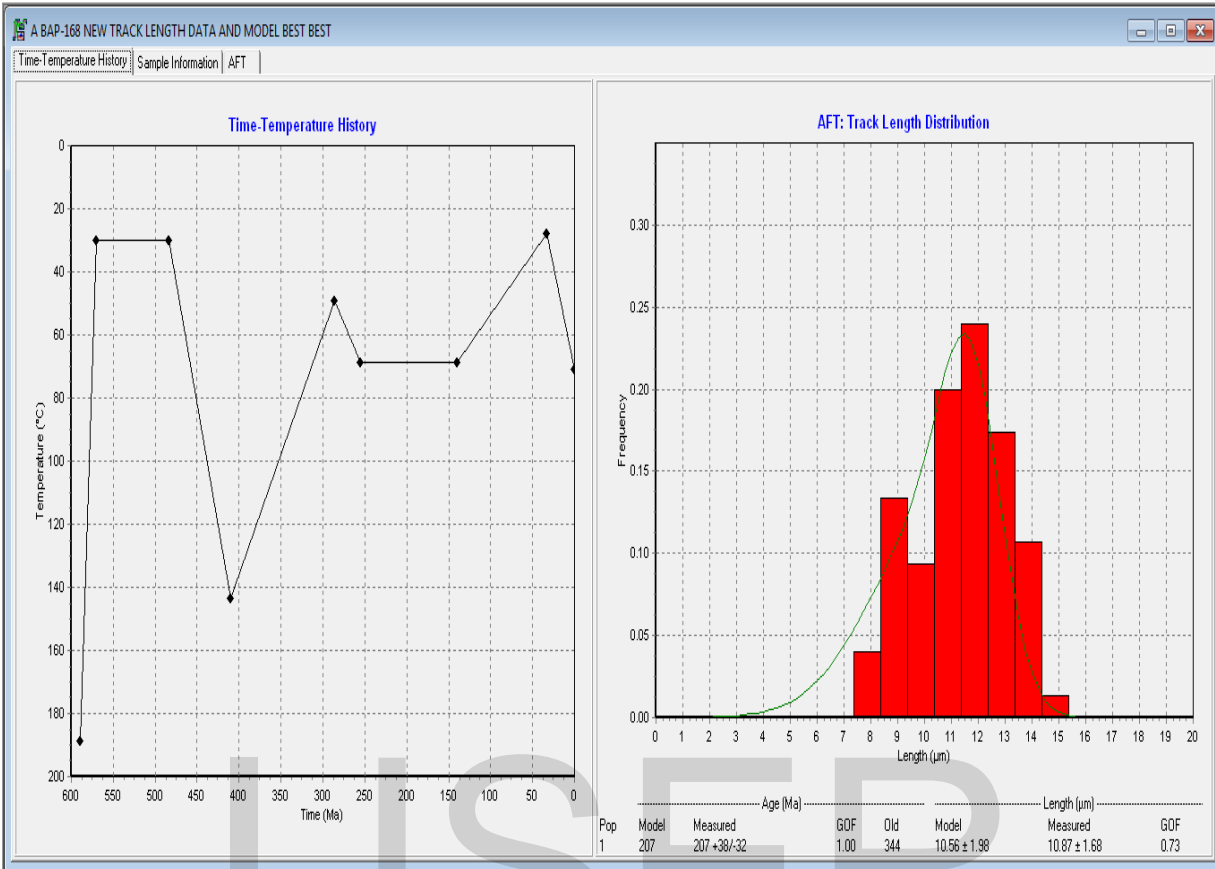
481

Model: 258	Model: 9.75 ± 1.96 µm
Measured: 258 +35/ - 31	Measured: 9.89 ± 1.58 µm
GOF: 1.00	GOF: 0.41

482

483

484



485

486

487

488

489

490

Sample Name: BAP – 168

491

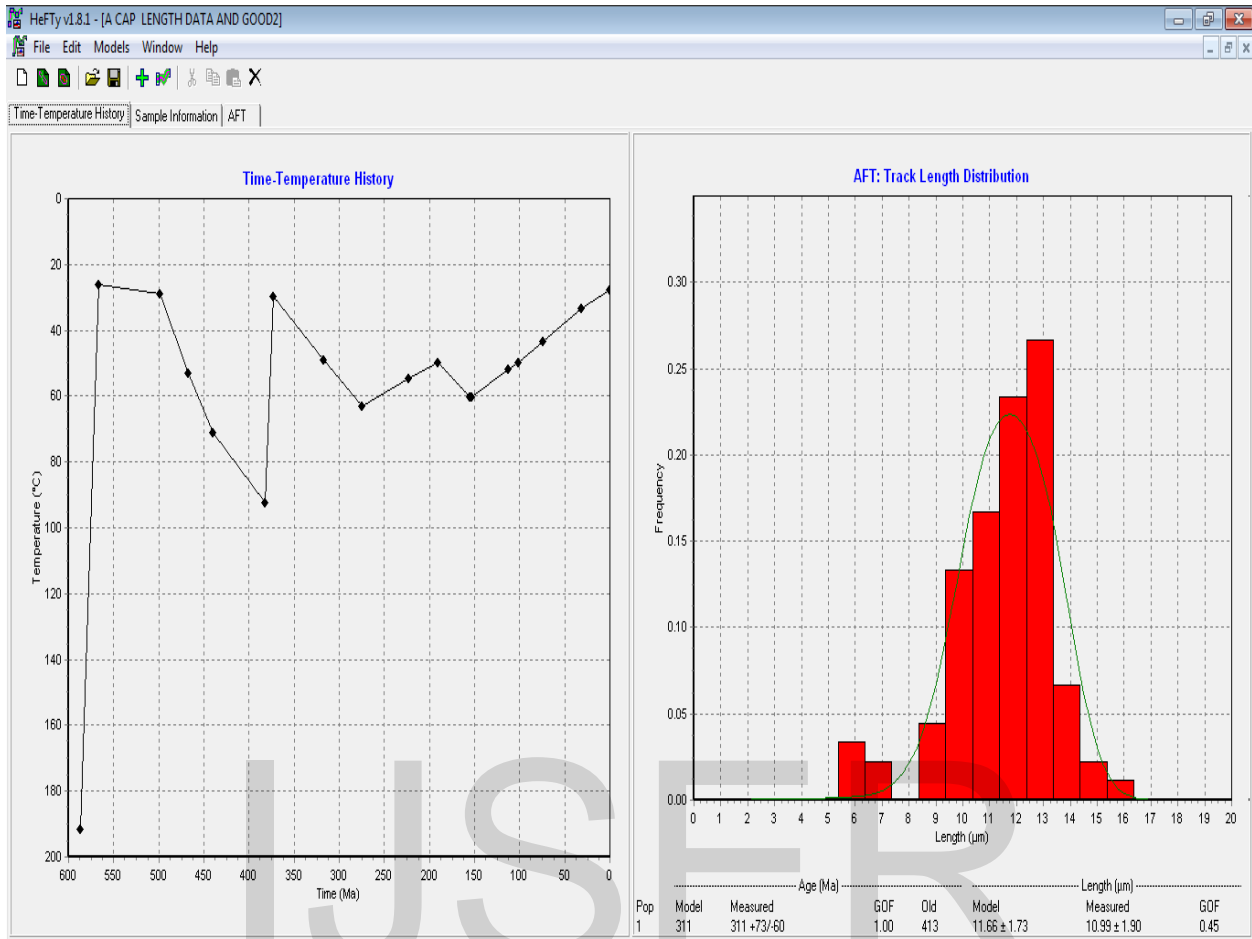
Model: 207	Model: 10.56 ± 1.98 μm
Measured: 207 +38 / -32	Measured: 10.87 ± 1.68 μm
GOF: 1.00	GOF: 0.73

492

493

494

495



496

497

498

499

500

501

Sample Name: CAP

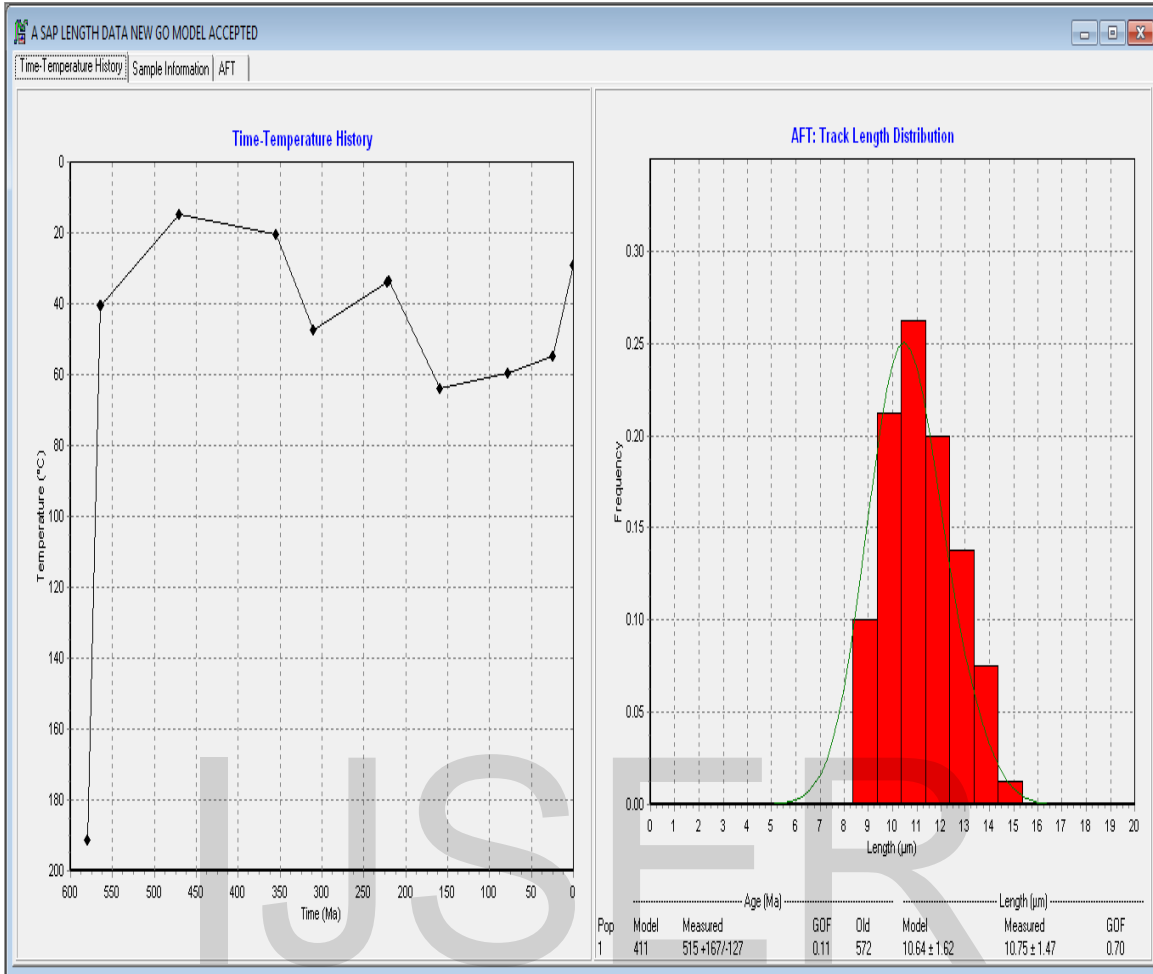
502

Model: 311	Model: 11.66 ± 1.73 µm
Measured: 311 + 73/ -60	Measured: 10.99 ± 1.90 µm
GOF: 1.00	GOF: 0.45

503

504

505



506

507

508

509

510

511

Sample Name: SAP

512

Model: 411	Model: 10.64 ± 1.47 µm
Measured: 515 +167 / -127	Measured: 10.75 ± 1.47 µm
GOF: 0.11	GOF: 0.70

513

514

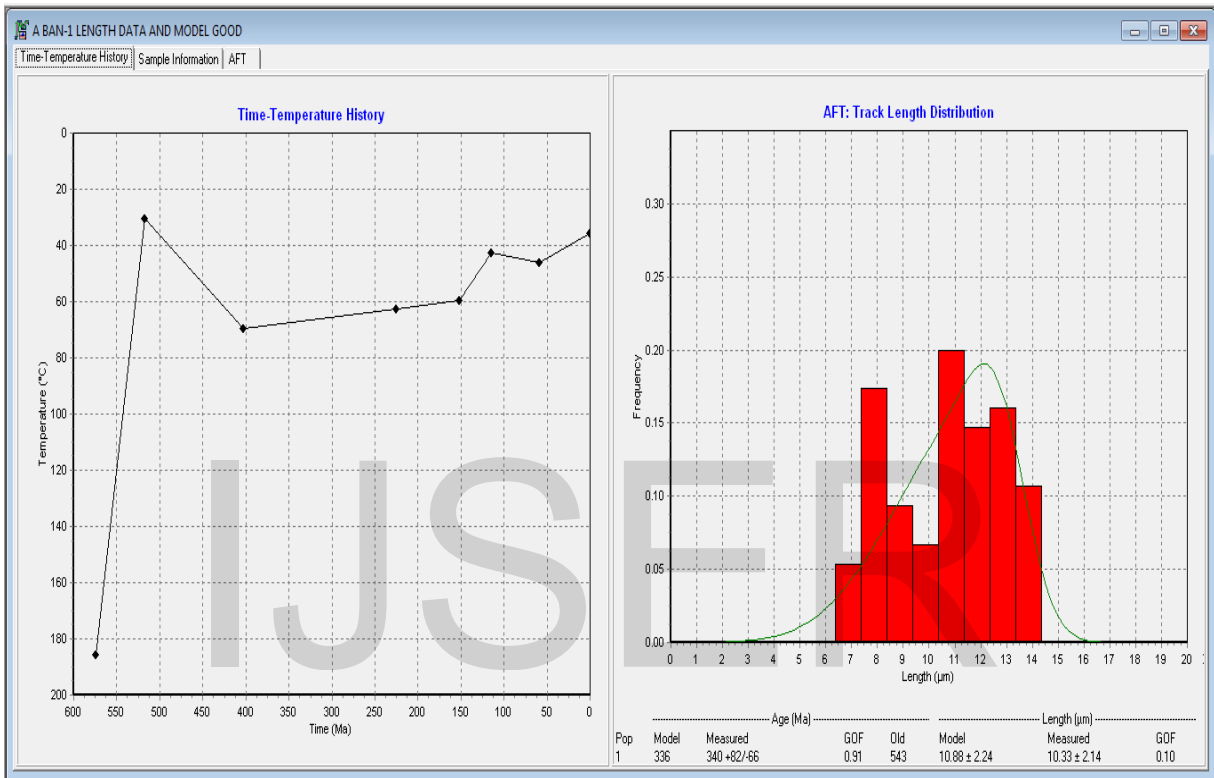
515

516

517

518

519 **Fig.5(b). Thermal History Models from Chhotanagpur Gneissic Complex**



520

521

Sample Name: BAN – 1

522

Model: 336	Model: 10.88 \pm 2.24 μm
Measured: 340 +82/- 66	Measured: 10.33 \pm 2.14 μm
GOF: 0.91	GOF: 0.10

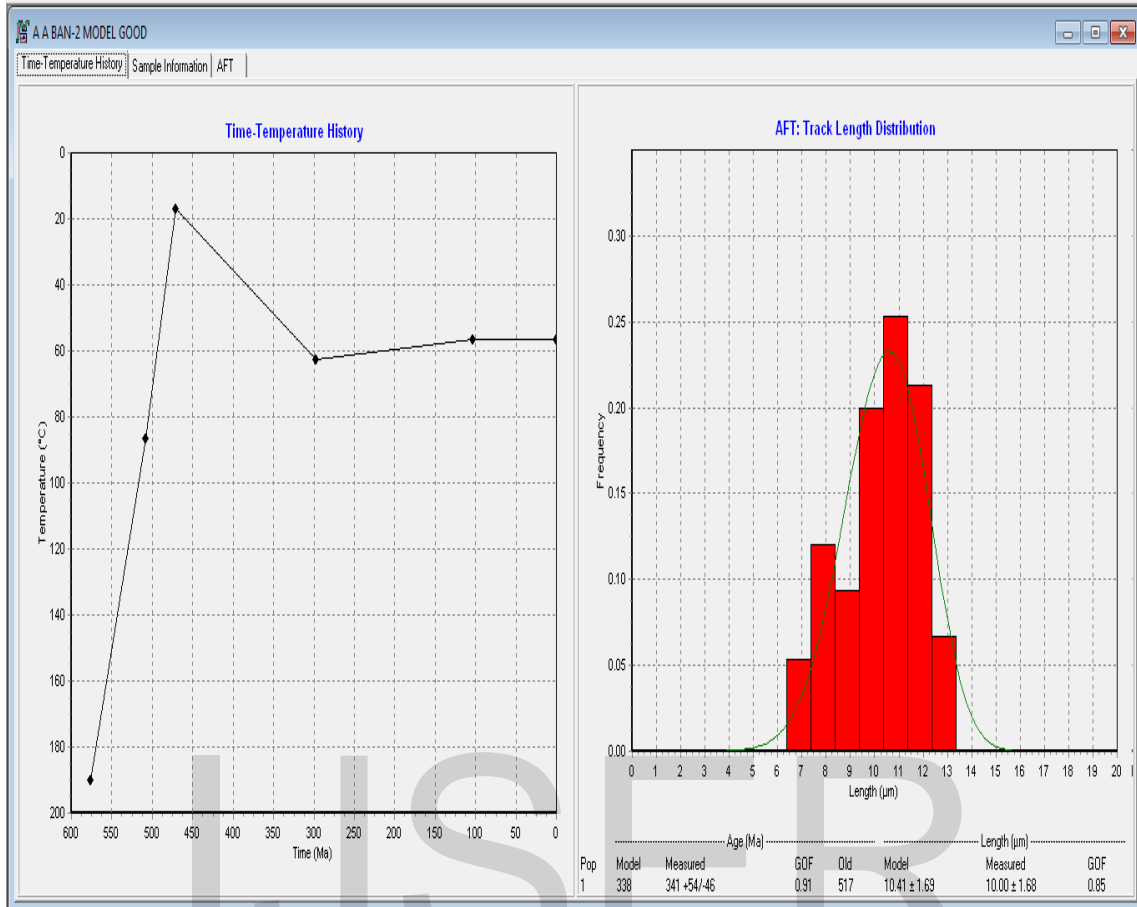
523

524

525

526

527



528

529

530

531

532

Sample Name: BAN – 2

533

Model: 338	Model: 10.41 ± 1.69 µm
Measured: 341 + 54/ -46	Measured: 10.00 ± 1.68 µm
GOF: 0.91	GOF: 0.85

534

535

536

537

538
539
540
541
542
543
544
545
546
547
548
549
550
551
552
553
554
555
556
557
558
559
560
561
562
563
564
565
566

Acknowledgements

I thank Prof. Barry Paul Kohn, “University of Melbourne”, Australia for his overall support and advice throughout my time as a Ph.D. student. He also sent me age standard minerals (Durango apatite) for zeta calibration, free of charge. Without his contribution, my work would have never been possible.

I thank Prof. Richard Ketcham “University of Texas”, U.S.A., who kindly reviewed my AFT models and provided valuable guidance for the improvement of the models.

Prof. Ketcham also kindly extended his help to offer the important interpretations of my AFT models and the offset AFT age. Prof. Ketcham sent me the copy of the most recent versions of the HeFTy (Ketcham, 2013, Version 1.8.1), free of charge.

I thank Prof. Paul B.O’ Sullivan, Apatite to Zircon, Inc., U.S.A., who kindly initiated my idea into the importance of obtaining the AFT data in the correct form. Prof. O’Sullivan also kindly advised me to contact Prof. Richard Ketcham.

My indebtedness to these professors knows no bounds.

I am highly indebted to the Director General of Geological Survey of India, 27, J.L. Nehru Road, Kolkata – 700 016, for his kind permission to perform my work in the laboratory of G.S.I, Kolkata.

I thank Mr. Partha Nag, Officer-in-Charge, WBMTDC, Purulia for his dedicated help with the field work.

I thank Mr. T.Ray Barman, Ex-Scientist, G.S.I, Kolkata, for his constructive advice.

567

568 Many thanks are due to the entire family of G.S.I., Kolkata, for their help and encouragement.

569

570 I thank the entire team of FRMII, Garching, Germany for providing me with use of the irradiation facility,
571 free of charge.

572 **Appendix-A**

573 The samples for this study were processed in the laboratory of the Geological Survey of India, Kolkata, after
574 obtaining permission from the Director General, GSI, Kolkata, West Bengal. The samples were prepared using
575 standard separation, grinding and polishing techniques. All the samples were prepared for the external detector
576 method. AFT mounts were etched with 70% HNO_3 at room temperature for 30 s and were irradiated in the thermal
577 facilities of FRM II at Garching, Germany together with dosimeter glass IRMM-540R (15ppm). Mica sheets were
578 etched using 48% HF at room temperature for 19 min. The fission tracks were counted under a total magnification
579 of 1000x. The calibrated area of one grid is $0.64 \times 10^{-6} \text{ cm}^2$. The length and D par were measured using a stage
580 micrometer and an ocular micrometer, with total magnification of 1000X.

581 Durango apatites were used as the age standard mineral, which was provided by Prof. Barry Paul Kohn, University
582 of Melbourne, Australia. A copy of the HeFTy software was provided by Prof. Richard Ketcham, Texas University,
583 U.S.A.

584 **Appendix B**

585 For modeling, 75 - 90 confined track lengths were used to fit the AFT data. 600 Ma is a reasonable starting point for
586 thinking about modeling and a hypothesis we attempted to test (Richard Ketcham, personal communication).

587 **References**

588 Acharya A, Basu S. K., Bhaduri S. K., Chaudhury B. K., Ray S., Sanyal A. K., 2006. Proterozoic Rock Suites along
589 South Purulia Shear Zone, Eastern India; Evidence for Rift-Related Setting. Geological Society of India, 68. 1069-
590 1086.

591 Basu S.K., Alkaline-Carbonatite Complex in Precambrian of South Purulia Shear Zone, Eastern India; Its
592 Characteristics and Minerals Potentialities. Indian Minerals, 47, 179-194.
593

594 Belton David X., Brown Roderick W., Gleadow A.J.W., Kohn Barry P, DOI: 10.2138/rmg.2002.48.16., Fission
595 Track Dating of Phosphate minerals and the Thermochronology of Apatite, 16, 579-630.
596

597

598 Bhattacharya D. K., Dasgupta S., Apatite Mineralisation along Singhbhum and Purulia-Bankura Shear Zones; their
599 Nature and Physico – Chemical Characteristics. Indian Minerals, 46, 123-132.

600

601 Brown R., Gallagher K., Johnson C.,1998. Fission Track Analysis and its Applications to Geological Problems.
602 Annual Review Earth Planet Science, 26, 519 - 572.

603

604 Carter A., Clift P. D., Dorr N., Gee D. G., Liskar F., Spigel C., Tebenkov A.M., 2012. Late Mesozoic – Cenozoic
605 exhumation history of northern Svalbard and its regional significance; constraints from apatite fission track analysis.
606 Tectonophysics, 514-517.

607

608 Geology and Mineral Resources of West Bengal. No. 30. Miscellaneous Publication, pp. 4-25.

609 O’Sullivan P. B., T. Tagami., Fundamental of Fission – Track Thermochronology, 58, 19-47.

610

611

612

613

614

615

616

IJSER

617

618

619

620

621

622

623

624

625

626

627
628
629
630
631
632
633
634
635
636
637
638
639
640
641
642
643
644

IJSER